



**HAL**  
open science

## High resolution data reveal fundamental steps and turning points in animal movements

Richard Gunner, Rory Wilson, Miguel Lurgi, Luca Borger, James Redcliffe, Emily Shepard, Mark Holton, Margaret Crofoot, Abdulaziz Alagaili, Samantha Andrzejaczek, et al.

### ► To cite this version:

Richard Gunner, Rory Wilson, Miguel Lurgi, Luca Borger, James Redcliffe, et al.. High resolution data reveal fundamental steps and turning points in animal movements. 2025. <hal-05195532>

**HAL Id: hal-05195532**

**<https://hal.science/hal-05195532v1>**

Preprint submitted on 1 Aug 2025

HAL is a multi-disciplinary open access archive for the deposit and dissemination of scientific research documents, whether they are published or not. The documents may come from teaching and research institutions in France or abroad, or from public or private research centers.

L'archive ouverte pluridisciplinaire HAL, est destinée au dépôt et à la diffusion de documents scientifiques de niveau recherche, publiés ou non, émanant des établissements d'enseignement et de recherche français ou étrangers, des laboratoires publics ou privés.



Distributed under a Creative Commons CC BY 4.0 - Attribution - International License



## High resolution data reveal fundamental steps and turning points in animal movements

Item Type	Preprint
Authors	Gunner, Richard;Wilson, Rory;Lurgi, Miguel;Borger, Luca;Redcliffe, James;Shepard, Emily;Holton, Mark;Crofoot, Margaret;Alagaili, Abdulaziz;Andrzejaczek, Samantha;Ariano-Sánchez, Daniel;Barbedette-Gerard, Thomas;Bennett, Nigel;Bernard, Alice;Brown, Rowan;Cole, Nik;Creel, Scott;Cruz-Neto, Arioaldo;Virgilio, Agustina di;Duarte, Carlos M.;Eizaguirre, Christophe;Elliott, Kyle;Faltusova, Monika;Garel, Mathieu;Gillies, Natasha;Gleiss, Adrian;Göppert, Aoife;Grémillet, David;de Grissac, Sophie;Guilford, Tim;Hoareau, Maxime;Jessopp, Mark;Gomez-Laich, Agustina;Miloš, Ježek;Lambertucci, Sergio;Marchand, Pascal;Marks, Nikki;Martins, Andréia;Meekan, Mark;Mizutani, Yuichi;Mortensen, Rasmus Mohr;Norman, Brad;Ortega, Josué;Padget, Oliver;Painter, Michael;Ponchon, Aurore;Provost, Pascal;Ponchon, Aurore;Quintana, Flavio;Reinhardt, Stefanie;Reynolds, Samantha;Rosell, Frank;Ruiz-Miranda, Carlos;Ryan, Peter;Scantlebury, Michael;Schoombie, Stefan;Scott, Rebecca;Silovský, Václav;Tatayah, Rabindra Vikash;Toïgo, Carole;Torrez, Lucia;Tremblay, Fred;Twining, Joshua;Yoda, Ken;Weimerskirch, Henri;Whelan, Shannon;Morales, Juan;Potts, Jonathan
Citation	Gunner, R., Wilson, R., Lurgi, M., Borger, L., Redcliffe, J., Shepard, E., Holton, M., Crofoot, M., Alagaili, A., Andrzejaczek, S., Ariano-Sánchez, D., Barbedette-Gerard, T., Bennett, N., Bernard, A., Brown, R., Cole, N., Creel, S., Cruz-Neto, A., Virgilio, A. di, ... Potts, J. (2024). High resolution data reveal fundamental steps and turning points in animal movements. <a href="https://doi.org/10.21203/rs.3.rs-5559169/v1">https://doi.org/10.21203/rs.3.rs-5559169/v1</a>
Eprint version	Pre-print
DOI	<a href="https://doi.org/10.21203/rs.3.rs-5559169/v1">10.21203/rs.3.rs-5559169/v1</a>
Publisher	Springer Science and Business Media LLC

Rights	This is a preprint version of a paper and has not been peer reviewed. Archived with thanks to Springer Science and Business Media LLC under a Creative Commons license, details at: <a href="https://creativecommons.org/licenses/by/4.0/">https://creativecommons.org/licenses/by/4.0/</a>
Download date	2025-08-01 07:52:48
Item License	<a href="https://creativecommons.org/licenses/by/4.0/">https://creativecommons.org/licenses/by/4.0/</a>
Link to Item	<a href="http://hdl.handle.net/10754/701808">http://hdl.handle.net/10754/701808</a>

# High resolution data reveal fundamental steps and turning points in animal movements

**Richard Gunner**

rgunner@ab.mpg.de

Max Planck Institute of Animal Behavior <https://orcid.org/0000-0002-2054-9944>

**Rory Wilson**

Swansea University

**Miguel Lurgi**

Swansea University <https://orcid.org/0000-0001-9891-895X>

**Luca Borger**

Swansea University <https://orcid.org/0000-0001-8763-5997>

**James Redcliffe**

Swansea University

**Emily Shepard**

Swansea University <https://orcid.org/0000-0001-7325-6398>

**Mark Holton**

Swansea University

**Margaret Crofoot**

Max Planck Institute of Animal Behavior

**Abdulaziz Alagaili**

King Saud University

**Samantha Andrzejczek**

Stanford University

**Daniel Ariano-Sánchez**

Universidad del Valle de Guatemala <https://orcid.org/0000-0003-4955-5018>

**Thomas Barbedette-Gerard**

Université Claude Bernard Lyon

**Nigel Bennett**

University of Pretoria

**Alice Bernard**

Université de Montpellier

**Rowan Brown**

<https://orcid.org/0000-0003-3628-2524>

**Nik Cole**

Durrell Wildlife Conservation Trust

**Scott Creel**

Montana State University <https://orcid.org/0000-0003-3170-6113>

**Ariovaldo Cruz-Neto**

Laboratório de Fisiologia Animal (LaFa)

**Agustina di Virgilio**

**Carlos M Duarte**

King Abdullah University of Science and Technology <https://orcid.org/0000-0002-1213-1361>

**Christophe Eizaguirre**

**Kyle Elliott**

McGill University

**Monika Faltusova**

Czech University of Life Sciences

**Mathieu Garel**

Office Français de la Biodiversité

**Natasha Gillies**

University of Liverpool <https://orcid.org/0000-0002-9950-609X>

**Adrian Gleiss**

Murdoch University

**Aoife Göppert**

Queen's University Belfast <https://orcid.org/0000-0002-9100-5717>

**David Grémillet**

CNRS-INEE <https://orcid.org/0000-0002-7711-9398>

**Sophie de Grissac**

CEBC CNRS

**Tim Guilford**

University of Oxford

**Maxime Hoareau**

Université de Lyon

**Mark Jessopp**

University College Cork <https://orcid.org/0000-0002-2692-3730>

**Agustina Gomez-Laich**

Instituto de Ecología, Genética y Evolución de Buenos Aires (IEGEB), CONICET

**Ježek Miloš**

Czech University of Life Sciences Prague <https://orcid.org/0000-0002-4127-9947>

**Sergio Lambertucci**

Grupo de Investigaciones en Biología de la Conservación, INIBIOMA (Universidad Nacional del Comahue - CONICET), Quintral 1250 (R8400FRF), Bariloche, Argentina <https://orcid.org/0000-0002-2624-2185>

**Pascal Marchand**

Office Français de la Biodiversité

**Nikki Marks**

Queen's University Belfast

**Andréia Martins**

Associação Mico-Leão-Dourado

**Mark Meekan**

Australian Institute of Marine Science

**Yuichi Mizutani**

Nagoya University

**Rasmus Mohr Mortensen**

Aarhus University <https://orcid.org/0000-0003-4975-608X>

**Brad Norman**

ECOCEAN

**Josué Ortega**

Max Planck Institute of Animal Behaviour

**Oliver Padget**

University of Oxford

**Michael Painter**

Czech University of Life Sciences Prague

**Aurore Ponchon**

CNRS-INEE

**Pascal Provost**

Réserve Naturelle Nationale des Sept-Iles

**Aurore Ponchon**

Green screen Festival e.V

**Flavio Quintana**

Instituto de Biología de Organismos Marinos (IBIOMAR-CONICET) <https://orcid.org/0000-0003-0696-2545>

**Stefanie Reinhardt**

University of South-Eastern Norway

**Samantha Reynolds**

School of Biological Sciences, The University of Queensland, St Lucia, QLD, Australia

<https://orcid.org/0000-0003-4094-8018>

**Frank Rosell**

Faculty of Technology, Natural Sciences and Maritime Sciences, Department of Natural Sciences and Environmental Health, University of South-Eastern Norway, 3800 Bø i Telemark, Norway

<https://orcid.org/0000-0003-1047-0156>

**Carlos Ruiz-Miranda**

Associação Mico-Leão-Dourado

**Peter Ryan**

University of Cape Town <https://orcid.org/0000-0002-3356-2056>

**Michael Scantlebury**

Queen's University Belfast

**Stefan Schoombie**

FitzPatrick Institute of African Ornithology, DST-NRF Centre of Excellence, University of Cape Town

<https://orcid.org/0000-0002-6566-0443>

**Rebecca Scott**

NERC

**Václav Silovský**

Czech University of Life Sciences Prague <https://orcid.org/0000-0001-6115-2516>

**Rabindra Vikash Tatayah**

Mauritian Wildlife Foundation

**Carole Toïgo**

Office Français de la Biodiversité

**Lucia Torrez**

Max Planck Institute of Animal Behaviour

**Fred Tremblay**

McGill University

**Joshua Twining**

Queen's University

**Ken Yoda**

Nagoya University <https://orcid.org/0000-0002-8346-3291>

**Henri Weimerskirch**

CNRS <https://orcid.org/0000-0002-0457-586X>

**Shannon Whelan**

McGill University

**Juan Morales**

INIBIOMA-CONICET, CRUB; San Carlos de Bariloche

**Jonathan Potts**

University of Sheffield

---

**Article**

**Keywords:**

**Posted Date:** December 18th, 2024

**DOI:** <https://doi.org/10.21203/rs.3.rs-5559169/v1>

**License:** © ⓘ This work is licensed under a Creative Commons Attribution 4.0 International License.

[Read Full License](#)

**Additional Declarations:** There is **NO** Competing Interest.

---

# Abstract

Animal movement paths display substantial complexity and variability, leading researchers to seek underlying rules that govern these patterns and mathematical models that best describe them. Using high-resolution ( $\geq 10$  Hz) movement from 43 vertebrate species across diverse taxa, mass, and lifestyles, we show that movement paths are universally composed of straight-line steps interspersed with sharp turns, echoing a pattern documented for lower taxa such as bacteria. We report how these vertebrate ‘fundamental step lengths’ and ‘fundamental turn angles’, which are intrinsically different from the straight-line paths detailed in studies using low resolution position data, vary with species’ mass, lifestyle, behaviour, and environmental context. To explain these, we posit that animals inherently move in a straight line until sensory information signals a perceived better heading, which instigates a turn. The constellation of fundamental step lengths and turn angles over varying time intervals affects how well different models of animal movement (such as random walk or Lévy flight) fit lower resolution data. By examining turns as decision points, we can seek drivers of animal movement patterns and thereby work to predict future paths under varying conditions.

## INTRODUCTION

The routes that self-propelled animals take as they move around their environment have fascinated and perplexed people for centuries<sup>1</sup>. Even today, understanding the drivers and rules behind animal path complexity and variability across scales remains a major challenge, particularly in vertebrates<sup>2,3</sup>. Fortunately, advances in animal-borne telemetry have made it possible to quantify movement of free-living vertebrates<sup>4</sup>, providing a basis for describing and modelling movement mathematically. The standard approach for describing animal trajectories uses straight lines to link locations acquired at relatively large sampling intervals (e.g. minutes to hours – but see Nathan, et al. <sup>5</sup>), generating movement ‘steps’, with corresponding turn angles between them<sup>6</sup>. This has produced results and theories that form the bedrock of much of quantitative animal movement ecology<sup>6</sup>. Nonetheless, such step lengths and turn angles remain an approximation of the true movement path and, lacking the necessary temporal resolution, it is unclear how much true animal paths are structured by real turns that occur within the ‘straight line’ sections<sup>7</sup>. We do know though, that animals turn for a variety of reasons, for example if constrained to do so by environmental structures or as they react to visual, chemical or auditory cues<sup>8</sup>. Indeed, the idea that animals might have their movement paths structured according to such sequential turn decisions is not new, with Aristotle suggesting that animal locomotion was based on ‘rational action’ over two thousand years ago<sup>1</sup>.

A fundamental feature of a turn is that it is normally brought about by an animal actively choosing to change its heading as it moves. As such, determination of animal heading with appropriate sub-second resolution should highlight all turns within any movement pathway. Accordingly, we used novel bio-logging sensors (magnetometers) to derive true path properties for 43 species, based on sub-second measurements of animal heading ( $\geq 10$  Hz). Our study taxa include fish, reptiles, mammals, and birds

that operate across the globe in highly varied habitats, and range in size from 0.3 to > 10,000 kg. We use these data to assess how sampling frequency affects the resultant path properties (step length and turn angle) and determine whether variation in “fundamental” step lengths and turn angles is linked to functional traits such as body size, movement medium and lifestyle. Finally, in a case study with a seabird, we demonstrate how the fundamental path properties can be used to predict space-use and movement trajectories.

## RESULTS

### Fundamental steps and turning angles

Key to our analysis is the temporal resolution of animal heading, derived from onboard magnetometers<sup>9</sup>, which, at 20 Hz (except for two species at 10 Hz, see Table S1), precludes the possibility of changes in trajectory going undetected. Such data offer an essentially continuous representation of animal movement, presenting a stark contrast to the traditional method that determines step lengths from sparsely spaced locations - usually once every five minutes to a few hours<sup>10</sup>. In the standard approach, multiple turns can be simplified into straight lines connecting infrequent, discrete locations, potentially smoothing out important details in the path<sup>7</sup>. We used a turn identification protocol<sup>11</sup> (for detailed methods see Supplementary text 2) that generally revealed what were visually obvious straight lines and turning points (Fig. 1A, B, C). We suggest that the associated step durations represent a precisely defined animal behaviour – maintenance of a specific heading during travel for a defined period – which we term ‘fundamental step durations’ ( $F_{\text{stepdurations}}$ ). These are not necessarily directly proportional to step ‘distances’ (lengths) commonly used in the literature although they equate directly if animals travel at constant velocity. The same principle applies to the angles of the identified turns, which we term ‘fundamental turn angles’ ( $F_{\text{turnangles}}$ ).

Newton’s First Law emphasizes the fundamentality of straight-line travel, stating that an object in motion continues to move in a straight line unless acted upon by a net external force. In our case, turning forces are produced by the animals, which explains why turns are energetically more costly than straight line travel<sup>12,13</sup> (see Supplementary text 3). So, all else being equal, straight line travel should be the most efficient mode of movement for animals<sup>14</sup>, also providing the shortest distance between two defined points and minimizing the number of turns. In keeping with expectations that selection pressure acts so that animals manage their energy expenditure optimally<sup>15</sup> and may also reduce cognitive load<sup>16</sup>, all species examined spent > 90% of their movement time travelling in straight lines (which we define as having an average deviation of less than 10% from a straight line – see Supplementary text 2), with 84% (36 out of 43 species) spending > 95% in straight-line trajectories (Fig. 1G).

Unsurprisingly, sections defined as ‘straight line’ were usually not perfectly straight<sup>6</sup> and followed one of two fundamental patterns of wobble (where we define “wobble” as the ratio between the mean deviation of a path segment from a straight line and the length of that line –  $e_k$  in Eq. 4 of Supplementary text 2).

There was a 'general baseline wobble' in most species (Fig. 1D), or the particular case of 'systematic wobble' in many procellariiform species, notably albatrosses, which manifested as a long, flat, sine wave-type pattern across 2D space (Fig. 1E). This is due to their dynamic soaring flight, which requires this pattern to extract energy from the wind and waves to minimize costs of transport<sup>17</sup>. In both wobble types, none of the species exhibited a mean wobble index above 0.05. Across all species, the mean wobble index was  $0.019 \pm 0.009$  ( $\pm 1$  SD), although there was appreciable variation between species (Fig. 1F). Thus, describing the paths between identified turning points as a straight line provided a good approximation to all observed tracks. The 'general baseline wobble' is presumably due to minimal navigational errors as well as animals being marginally affected by conditions *en route*, such as gusts of wind for flying birds or minor changes in substrate or topography for terrestrial animals<sup>18</sup>.

$F_{\text{stepdurations}}$  varied substantially within and between species, but frequency distributions were all left-skewed and unimodal, even when viewed on a log scale (Fig. 2A). Mean step duration varied between 12 s (European pine marten, *Martes martes*) and 54 s (whale shark, *Rhincodon typus*), and were species-specific (Fig. 2B). Mean step duration increased with animal mass except for flying birds (Fig. 2C): Linear regression revealed strong and significant positive relationships for terrestrial (intercept = 2.608, slope = 0.234 [scaling exponent = 0.102],  $R^2 = 0.458$ ,  $p < 0.001$ ) and aquatic species (intercept = 2.738, slope = 0.314 [scaling exponent = 0.136],  $R^2 = 0.791$ ,  $p = 0.018$ ) but no relationship for aerial species (intercept = 2.885, slope = 0.144 [scaling exponent = 0.062],  $R^2 = 0.021$ ,  $p = 0.625$ ).

Importantly, the relationship between step durations and turning rates (rate = 1/duration) meant that turning rates were higher in smaller terrestrial- and aquatic species. This is presumably because larger animals have decreased mass-specific muscle force<sup>19</sup> so activities that require high mass-specific power, such as climbing<sup>20</sup> or turning<sup>21</sup>, result in them having a higher increment in energy expenditure than smaller animals<sup>22</sup>, particularly when turns are acute and/or fast<sup>23</sup>. This rationale has been used to explain the radical differences in athleticism routinely adopted by animals of different masses<sup>22</sup>. Notably, while well-established relationships between animal mass and various biomechanical parameters, like stride length and maximum speed, typically have scaling exponents greater than about 0.3, our findings for scaling exponents for step duration - which inversely relates to turning rates - were considerably lower for both terrestrial and aquatic species. Specifically, the scaling exponent for step duration in terrestrial species is about three times lower than this benchmark, and for aquatic species about two times lower, suggesting a marked deviation from the typical biomechanical trends. These significant relationships underline a slower increase in step duration (and hence a faster turning rate) with increasing size than is commonly observed for other biomechanical parameters. The difference may illustrate the extent to which biomechanics relates to aspects of behavioural choice, particularly as concerns decisions to turn. We suggest that animals pursuing prey or being pursued themselves would indeed have scaling exponents much closer to those describing biomechanical parameters noted in the literature. The smaller exponent detected here likely reflects the reduced extent of high-performance activities in our data because most turns will not be high performance. In addition, the observed trends (Fig. 2C) may stem from larger animals requiring more definitive cues to undertake turns due to their

relatively higher energetic cost of execution (Supplementary text 3). This would lead to their generally reduced incidence although, since the  $F_{\text{stepduration}}$  is remarkably consistent across a massive range of body size (Fig. 2C), the case is far from compelling. The lack of a trend in step duration (and turning rate) in flying animals may be because all the large bird species (> 1.5 kg) in our study use soaring flight which requires regular changes in heading to extract energy from the environment, i.e. during thermal and dynamic soaring<sup>24</sup>. This increases their turning rate disproportionately relative to mass. The inclusion of large, obligate flapping bird species such as geese may alter this outcome.

In absolute terms, the identification of turns is important because they are not only energetically costly<sup>12,13,21</sup>, but fundamental turns should represent decision points, where specific inputs have elicited a change in heading<sup>7,25</sup> resulting in movement to a different environmental space than if the animal had not turned. Specifically, animals can incur the energetic costs of turning because the likely fitness benefits of turning outweigh those of continuing in a straight line. Laboratory maze work tells us that paths taken are driven by animal choice at every turn<sup>26</sup>. Similarly, animals free to move in two or three dimensions, from insects to sharks, follow odour plumes to their source, altering heading in relation to changing odour density<sup>27</sup>. Wild birds follow tactile and visual cues over mm and km scales, respectively<sup>8</sup>. This highlights the value of identifying true turns, as it allows them to be linked to environmental predictors over different scales, recognizing that the way animals respond to perceived cues (including social information<sup>28</sup>) will be modulated by past experiences and their internal state such as changing levels of hunger<sup>3</sup>.

The value of identifying turns is not just applicable to locating resources *per se* though. Although a small proportion of turns may occur due to 'spontaneous behaviour' such as play<sup>29</sup>, we expect many turns to occur when animals move around obstacles in cluttered environments, change heading to exploit sources of environmental energy (such as birds in thermals<sup>30</sup>), and during execute escape manoeuvres from predators<sup>23</sup>. Indeed, not only do obstacles induce turns, but they can also dictate prolonged straight-line movement. For instance, the presence of barriers like fences, walls, roads, and streams can constrain animals to travel 'along' them until they encounter a break, permitting a turn. These confounding factors may tend to weaken relationships between turn angle and animal mass because the spatial distribution of environmental cues (e.g. the location of obstacles or food) that elicit (or prevent) turns is not expected to be animal mass-dependent. This, together with the wide variety of behaviours that the movement data encompasses, could contribute to the variability in the relationship between  $F_{\text{turnangle}}$  and mass (see also Table S3).

## A simple rule-based framework for interpreting animal movement

Based on our empirical observations, we propose a simple framework to explain animal movement. On initiating a particular movement behaviour driven by internal state, such as foraging elicited by hunger<sup>3</sup>, an animal chooses its heading relative to the proximate goal<sup>3</sup> by following a straight line. The animal's

path continues along this line while the animal continuously samples environmental cues or other sources of information, such as reactions to physical obstacles, to conspecifics, and other species<sup>31,32</sup>. We also expect changes in direction to be modulated by memory which could be triggered by environmental features<sup>33</sup> or shifting internal state<sup>3</sup>. Once a change in trajectory appears beneficial, the animal turns to the new heading and repeats the process. Given that movement associated with different behaviours requires responses to different cues (e.g. foraging behaviour versus navigation back to a central place), we expect different 'movement behaviours' to result in different compositions of  $F_{\text{stepdurations}}$  and  $F_{\text{turnangles}}$ .

In his seminal work on animal movement, Turchin<sup>6</sup> states 'many organisms tend to move relatively straight for a period of time, and then make a turn and move in another direction'. He underpins this with examples using prokaryotes and invertebrates with limited cognitive complexity ranging from bacteria to insects although he gives an example of a single bird. But our work now provides empirical evidence to demonstrate that this premise holds for all the vertebrates we examined, covering fish, reptiles, mammals and birds. This framework is fundamentally different from classic movement models because, instead of incorporating random elements as a convenience<sup>34</sup>, it ascribes path changes to choices based on external cues (or state changes), which may serve as attractors or repellers (of variable importance)<sup>25,35</sup>. The range over which diverse animal sensory systems operate, even within one species<sup>3</sup>, and the distribution of available cues over space and time is what determines the overall path structure *via* step lengths that are curtailed by the animals' angular responses to these cues.

This approach applies a precise formulation to the development of animal paths, emphasizing that minor adjustments in turn angle can significantly influence downstream space usage. Although such decision-based movement can, over a long period of time and with enough data, have similar statistical features to diffusive movement (i.e. mean square displacement scaling with time), very different paths can exhibit the same coarse features. For example, individual random walks with the same underlying random process can end up taking very different individual trajectories. Similarly, different animals could display movement patterns that resemble diffusive (or possibly super-diffusive) properties over extended durations. However, such observations provide limited insight into the specific nature of their trajectories, the precise locations they traverse, or the underlying reasons for their movement patterns. On the other hand, if we consider fundamental turning points as decision markers, it encourages us to examine an animal's movement behaviour both before and after these fundamental turns. This can provide insights into the motivation or urgency behind each turn. A clear illustration of this concept is a predator like a cormorant (a marine bird that forages underwater) altering its path upon sighting pelagic prey (e.g. Fig. S6).

It would be illusionary to expect to be able to infer the reasons for all turns in our data due to the large number of cues appealing to diverse sensory systems that might elicit an animal to turn. However, some cases appear clear, including, but not limited to: (i) animals that turn to extract energy from a positive energy landscape<sup>18</sup> (Fig. 3A); (ii) animals faced with an obstacle that hinders or blocks movement

(Fig. 3B); (iii) turns made by arboreal animals that have to choose between alternative branches in a manner analogous to rats in a maze (Fig. 3C); (iv) species that use area-restricted search<sup>36</sup> to exploit patchy prey changing from 'searching' to 'exploiting' behaviour<sup>32,37,38</sup> (Fig. 3D); (v) animals that turn to reduce overall power requirements for movement in energetically onerous terrain (Fig. 3E); and (vi) animals pursued by predators that execute acute, fast turns to enhance their chances of escape<sup>23</sup> (Fig. 3F). As part of this, we expect, and observe, how  $F_{\text{stepduration}}$  and  $F_{\text{stepduration}}$  (or  $F_{\text{turnfrequency}}$ ) change over space as environmental context changes (Fig. 3G). These may also be different for animals moving in groups.

Importantly, being able to observe  $F_{\text{stepdurations}}$  and  $F_{\text{turnangles}}$  means that we have access to the true points at which animals alter their paths, which is a first step to recognizing turn elicitors (Fig. 3A-F) and a critically important part of understanding what structures animal paths. This makes a case for plotting turn points in space to help understand how movement patterns relate to the environment, which we consider to be a key aspect of studying animal behaviour, ecology and conservation<sup>35</sup>. Spatial clustering of particular step-lengths is already commonly used, e.g. to identify likely feeding areas, associated with area-restricted search behaviour (ARS)<sup>37</sup>. Georeferencing  $F_{\text{turnangles}}$  goes beyond this, allowing scientists to link true turn points to specific, and potentially fine-scale cues (e.g. Figure 3G).

## Frequency distributions of F and their relationship to F

Many animal movement models adopt random turn angles between steps<sup>40</sup> and so have a predicted uniform step angle distribution between 0 and 360°. We show that there is support for this when using turn angles derived from locations determined at typical sampling frequencies<sup>7</sup>, although there is no support for uniformly distributed turn angles in highly resolved movement data (Fig. 4A, B). In fact, turn angle magnitude follows a truncated gamma distribution (Table S4, Fig. S5). This indicates a fundamental difference between quantifying animal movement based on  $F_{\text{turnangles}}$  from high-frequency, continuously sampled data compared to estimates derived from temporally spaced discrete location data (*cf.* black versus colored lines in Fig. 4A). Critically, it would seem that the constellation of  $F_{\text{stepdurations}}$  and  $F_{\text{turnangles}}$  over space according to behaviour will affect how well different models of animal movement fit lower resolution data. In support of this, we note how many fish have best-fit models of movement that are best classified by either Brownian or Lévy depending on environmental context, including species that switch as they move across habitats<sup>41</sup>.

How turn angles interact with step durations/lengths is important in shaping movement paths and, in a manner similar to that reported for sparse location data<sup>42</sup>, we detected a correlation between  $F_{\text{stepdurations}}$  and  $F_{\text{turnangles}}$  for many species (73%, Fig. 4C, D, Table S5). The proportion of terrestrial (and arboreal) species with significant correlations (60%) was significantly lower than the combined proportion for aerial (93%) and aquatic (83%) species, respectively (95%;  $\chi^2 = 4.34$ ,  $p < 0.05$ ). We suggest this is due to landscape features continually interrupting what would otherwise be longer straight-line

step lengths for terrestrial animals. This would occur much less in aerial or aquatic species, and certainly in our constellation of species, although it could occur in marine benthic organisms too.

Where correlations between step durations and turn angles do occur, they could be driven by specific behaviours<sup>42</sup>. For example, animals engaged in directed travel should have long step durations and small turn angles. Short step durations and more acute turn angles would, on the other hand, be expected when animals exploit patchy food resources<sup>42</sup>. Since we assume that, at any given moment, animals adopt specific, single behaviours, the distribution of turn angles and step durations should therefore vary over time as animals switch from one behaviour to another. Our data typically show this, with both  $F_{\text{stepduration}}$  and  $F_{\text{turnangle}}$  distributions changing over time, and consequently space, across species (e.g. Figure 5A). Indeed, for 30 species, we found that the change in turning angle distribution over time was significantly different from that exhibited by random fluctuations, exemplified by repeatedly drawing from a uniform distribution (Fig. 5B, evidenced by the confidence intervals not intersecting with the 50% mark along the y-axis; see Supplementary text 2 for detailed methodology). The other 13 species still show visual changes in turning angle distribution over time, but our techniques were unable to distinguish these changes from those that might occur randomly from an animal turning uniformly at random. Interestingly, of the five arboreal species analysed, four exhibited 95% confidence intervals that did not intersect the upper boundary - represented by the dashed line - with the semi-arboreal white-nosed coati, *Nasua narica*, also positioned near the boundary of this confidence interval (Fig. 5B). This phenomenon is marked by consistently larger turning angles compared to those expected under a uniform-random turning model. Such behaviour might be particularly prevalent among dynamic arboreal animals that frequently execute large directional shifts in the upper strata of wooded habitats, due to the constraints imposed by the connectivity of the canopy<sup>43</sup> (Fig. 3C). Note also, that the great frigatebird, *Fregata minor*, has the highest degree of straight-line wobble (Fig. 1F) and the lowest proportion of straight-line travel of any of our species (Fig. 1G). This species, along with the Andean condor, *Vultur gryphus*, is heavily dependent on local thermals and so must spend a substantial amount of time turning and gaining altitude within them.

## Predicting animal movement

A vital aspect of understanding animal movement lies in our ability to predict animal paths under varying conditions, including future scenarios<sup>44,45</sup>. This requires the movements of an animal to be documented as a sequence of behavioural responses to spatially varying conditions. Our theory suggests that the interplay between  $F_{\text{stepduration}}$  and  $F_{\text{turnangle}}$  distributions is indicative of varying travelling behaviours, revealing how these distributions respond to particular spatial conditions (see Fig. 3G). However, while these distributions provide valuable insights, they alone cannot independently generate realistic movement paths due to the absence of overall directionality.

To address this, we used an agent-based model<sup>46</sup> that integrates highly resolved empirical data. By imposing general headings on projected movement path sectors—based on prior observations of animal

movements where headings are associated with  $F_{\text{stepduration/length}}$  and  $F_{\text{turnangle}}$  distributions—the model more closely resembles real-world paths. An example using Magellanic penguins foraging for their chicks illustrates this approach. These penguins operate in open seas, with no obstacles and minimal predators, making their turning decisions largely driven by prey availability and navigation needs. Real data also show where prey are caught (Supplementary text 4) enabling metrics for prey density to be allocated to specific spatial cells. These cells are then linked to the corresponding distributions of  $F_{\text{stepdistances/lengths}}$ ,  $F_{\text{turnangles}}$  and heading, allowing predictions of foraging success.

Our time- and space-specific distributions of  $F_{\text{stepdistances}}$  and  $F_{\text{turnangles}}$  used in our agent-based model gives significantly better alignment with patterns observed in actual penguin tracks and markedly higher prey harvesting rates than conventional animal movement models (correlated random walk and Lévy flight; Fig. 6A). Importantly, observed changes in  $F_{\text{stepdistance}}$  and  $F_{\text{turnangle}}$  distributions in relation to prey density facilitate the prediction of movements under various ‘what if’ scenarios. For instance, in the case of the foraging penguins in Fig. 6, altering prey densities across foraging areas (see Supplementary text 4 for details) allows explicit predictions about the spatial extent the model birds will utilize (Fig. 6C), with important implications for time and energy expenditure<sup>45</sup>.

Our proposal that agent-based models can utilize  $F_{\text{stepdurations/distances}}$  and  $F_{\text{turnangles}}$  to predict animal movement can be further refined because  $F_{\text{turnangles}}$  may reflect behavioural responses as animals move toward attractants or away from repellents<sup>25</sup> (Figs. 3G, 5A). Specifically, incorporating both incentive and repulsion mechanisms into models can enhance our understanding and prediction of how wild animals react to specific features such as roads<sup>47</sup> or wind turbines<sup>48</sup>. This approach may also aid in developing cues to guide animals away from known threats. In our increasingly human-perturbed world, such refinements are pivotal for assessing the consequences of conservation-oriented interventions, thereby contributing to species protection and persistence<sup>44</sup>.

Our approach provides a compelling alternative to Step Selection Functions (SSFs) by focusing on intrinsic movement metrics —such as natural step lengths, turn angles, and directional headings — directly derived from empirical data. Unlike SSFs, which often assume static, environment-driven choices<sup>49</sup>, our model dynamically adjusts movement at a fine scale, accommodating both spatial and temporal variations inherent in real animal behaviour. By grounding movement in core behavioural metrics rather than contextual habitat associations, this method more accurately captures the continuity and directional persistence of animal paths. Consequently, it provides a more biologically realistic model that is both temporally responsive and spatially detailed. This adaptability is particularly valuable for understanding movement in complex or fluctuating environments, where rigid, static models may fail to account for critical aspects of animal navigation.

Overall, we propose that the discovery that there are species-, behaviour- and environmentally specific  $F_{\text{stepdurations/lengths}}$  and  $F_{\text{turnangles}}$  has significant implications for our understanding of animal movements. This finding not only deepens our understanding of why animals move as they do but may

also enhance our ability to predict their behaviour under changing conditions. In fact, trait-linked patterns in  $F_{\text{stepdurations/lengths}}$  and  $F_{\text{turnangles}}$  may ultimately allow us to project what species are expected to do even in the absence of direct movement data (*cf.* Table S4, Fig. S5). To date, researchers have made remarkable progress in understanding animal movement using techniques that are temporally constrained, with movement ‘steps’ dictated by technological limitations<sup>50</sup>. However ongoing advancements in instrumentation<sup>51</sup> now enable us to determine the ‘steps’ decided by the animals themselves, providing the potential for a greater understanding of the underlying movement rules.

## METHODS

### Data and code availability

### Tag deployment details and analysis

We deployed Daily Diary (DD) tags<sup>52</sup> on 43 species (15 birds, 3 fish, 3 reptiles and 22 mammals) covering a size range of 0.3–10,000 kg to obtain data on their movement patterns. The tags contained tri-axial magnetometers, tri-axial accelerometers and pressure sensors<sup>52</sup>, allowing travel headings over time to be deduced<sup>9</sup>. Sampling rates ranged from 10 to 40 Hz, and derived tracks were sub-sampled to either 10 or 20 Hz for analysis. See Table S1 for detailed information on sampling rates, sample size, locations, and deployment dates. Refer to Supplementary text 1 for ethical approvals, funding sources, and acknowledgments pertaining to each species.

Tag data were first processed to exclude periods immediately following the tagging process to minimize the probability of potential tagging effects; this exclusion period typically lasted a few days. Data were then examined to identify extended periods of active movement (excluding non-travelling movement behaviour), noting the travel medium, air, water or on land. From these periods, a single continuous segment (usually between 5 and 36 h) was analyzed per individual animal. The variation in duration was entirely due to the variation in activity patterns among species. For example, pine martens were typically only continuously active for a few hours a day, whereas sharks swam continuously. The compass and acceleration data were used to calculate headings following methods described in Gunner et al.<sup>9</sup>. Additionally, for select case studies, absolute animal locations over time were determined via dead-reckoning, incorporating periodic verified locations obtained through co-deployed GPS to correct for drift<sup>10</sup>. In these instances, fundamental step distances/lengths ( $F_{\text{stepdistances/lengths}}$ ) could be used to quantify movement patterns.

Variations in turns within the heading data were identified using the protocol defined by Potts et al.<sup>11</sup>. These variations ranged from an average minimum of 10 turns per hour across individuals for whale sharks to an average maximum of 207 turns per hour for the European pine marten. Briefly, the algorithm detects changes in the heading by sliding a small window across the time-series of headings and calculating the squared circular standard deviation (SCSD) within the window. Spikes in SCSD indicate

turns, and candidate turns were filtered based on achieving a threshold turn angle of  $30^\circ$  for all species<sup>7,11</sup> within a species-specific time window (see Potts et al.<sup>11</sup> and Supplementary text 2 for details).

## Agent-based modeling

We developed an agent-based model to predict the foraging movement paths of Magellanic penguins (*Spheniscus magellanicus*) foraging at sea, by utilizing empirical data from GPS-corrected dead-reckoned tracks of 27 individuals, including fundamental step length ( $F_{\text{stepdistance}}$ ), turn angle ( $F_{\text{turnangle}}$ ), and associated compass heading ( $H$ ). The foraging landscape was divided into equally spaced grid cells with a resolution of  $10 \text{ km}^2$ , enabling the calculation of unique frequency distributions (Empirical Cumulative Distribution Functions, ECDFs) for  $F_{\text{stepdistance}}$ ,  $F_{\text{turnangle}}$ , and  $H$  within each grid cell. These distributions were further segmented by journey phase, defined as either outbound or inbound. The transition from outbound to inbound was identified by the onset of a continuous downward gradient in the penguins' cumulative shortest distance to the colony. At the beginning of the simulation, each agent's movement parameters ( $F_{\text{stepdistance}}$ ,  $F_{\text{turnangle}}$ , and  $H$ ) were initialized based on the outbound ECDF distributions from the grid cell corresponding to their departure point near the colony. Each agent navigated a virtual 2D spherical coordinate system. At each time step,  $F_{\text{stepdistance}}$  and  $F_{\text{turnangle}}$  were randomly drawn from their respective ECDFs, and the direction of each turn was selected to align with the sampled  $H$ . At each movement step, the agent was dead-reckoned using this information to recalculate its geographical position and cumulative (Haversine) distance traveled. Upon entering a new grid cell, the agent recalibrated its  $F_{\text{stepdistance}}$ ,  $F_{\text{turnangle}}$ , and  $H$  distributions using the ECDF data specific to that grid cell. When the cumulative distance reached a user-defined proportion of the maximum distance threshold, the agent updated its grid cell ECDF information to reflect the inbound phase of the foraging trip. The simulation continued until each agent had traversed a user-defined total cumulative distance traveled. The R code for this model is available as a customizable function on GitHub [[https://github.com/Richard6195/Agent-Based\\_Fundamental\\_Steps\\_and\\_Turns\\_Simulation-](https://github.com/Richard6195/Agent-Based_Fundamental_Steps_and_Turns_Simulation-)]. Users can specify options, including (but not limited to) restricting the  $F_{\text{stepdistance}}$  and  $F_{\text{turnangle}}$  distributions to a specific quantile range, adding first-order autocorrelation to movement metrics, refining journey-phase segmentation of grid-cell ECDFs, filling empty grid cells with information from neighboring grids within a given radius or from global distribution values, and selecting from multiple heading adjustment strategies to balance turn angle and heading.

## Declarations

### Data and code availability

On publication, data will be available on Dryad repository [<https://doi.org/10.5061/dryad.gxd2547sd>]. Agent-based modelling R code available on Github [[https://github.com/Richard6195/Agent-Based\\_Fundamental\\_Steps\\_and\\_Turns\\_Simulation-](https://github.com/Richard6195/Agent-Based_Fundamental_Steps_and_Turns_Simulation-)].

## ACKNOWLEDGEMENTS

Please refer to Supplementary text 1 for specific acknowledgments, ethical approvals, and funding sources (in addition to those listed below) related to each species analysed in this study. This work was supported by Ailes Marines (DG), the Department for Economy Global Challenges Research Fund grant (DMS). The Beveridge Herpetological Trust and Durrell Conservation Trust, International Association of Avian Trainers & Educators (IAATE) and the ANCYPT grant PICT 2021-I-A-00484 (SAL), by Researchers Supporting Project RSPD2023R602, from King Saud University, the Deanship of Scientific Research at the King Saud University through Vice Deanship of Research Chairs (AA), the Royal Society/Wolfson Lab refurbishment scheme (RPW), the Royal Society for the Protection of Birds and the South African National Antarctic Programme (PGR), the Biotechnology and Biological Sciences Research Council (BBSRC), grant BB/M011224/1 (NG), the NSERC Discovery Grant and the European Research Council under the European Union's Horizon 2020 research and innovation program, grant 715874 (ELCS), the Argentine fund for scientific and technological research (FONCyT), grant PICT 2015 0815 (JMM), the Department of Agriculture, Environment and Rural Affairs, Northern Ireland (DMS), the Royal Norwegian Society of Sciences and Letters Special (FR), the Challenge Fund and Newry, Mourne and Down District Council, the College of Science Santander Travel Grant, the European Research Council Advanced Grant under the European Community and 39th Seventh Framework Program FP7/2007–2013, grant ERC-2012-ADG\_20120314 (HW), the National Agency for Science Promotion, grant PICT 2018-01480 and PICT 2017-1996, under the aegis of the Ministerio de Ciencia, Tecnología e Innovación Productiva, Argentina (FQ), the First Trust Travel Scholarship, Queens University Belfast (AG), the Max Planck Institute for Animal Behaviour's Department for the Ecology of Animal Societies (directed by MC), the Future Ocean Cluster of Excellence grant CP1217 (RS), the National Geographic grant GEFNE69-13 (CE), the Whitley Wildlife Conservation Trust (CE), the Future Ocean Capacity Building (CE), the King Abdullah University of Science and Technology (KAUST) under the KAUST Sensor Initiative (led by CMD), the European Regional Development fund through the Ireland Wales Co-operation Programme, the University Grant Competition at the Czech University of Life Sciences in Prague, grant 82/2021, the Ministry of Agriculture of the Czech Republic, the OP RDE project Improvement in Quality of the Internal Grant Scheme at CZ, grant CZ,.02.2.69/0.0/0.0/19\_073/0016944, the "EVA4.0" grant CZ,.02.1.01/0.0/0.0/16\_019/0000803 financed by OP RDE, and supported by "NAZV" grant QK1910462, the Crowdfunding campaign on the Experiment platform (doi:10.18258/7190), the Holsworth Wildlife Research Endowment, the UWA Graduate Research School for fieldwork, the Australian Institute of Marine Science, the Japan Society of the Promotion of Science through Grants-in-Aid for Scientific Research, grants 16H01769, 16H06541, 22H00569, 21H05294, the JST CREST grant JPMJCR, Japan (KY), the Estate of the late Winifred Violet Scott, the Jock Clough Marine Foundation, Rolex Awards for Enterprise (RPW, BN), the MG Kailis Group (BN), RAC Parks and Resorts (BN), the National Science Foundation, grants IOS1145749 and DEB-2032131 (SC), the National Geographic Society Big Cats Initiative, the Gemfields Inc World Wildlife Fund– Netherlands & Zambia, the Bennink Foundation, Painted Dog Conservation Inc, Rob and Kayte Simpson, Prabha Sarangi and Connor Clairmont, Wilderness Wildlife Trust, Tusk Trust, Panthera, Elephant Charge, Ntengu Safaris, the IUCN Save Our

Species/European Union, and the European Research Executive Agency (REA) for providing support for the analysis (cross-species) Project 101060072 – ACTNOW.

## AUTHOR CONTRIBUTIONS

Conceptualization: RPW and RMG. Methodology: All authors. Investigation: RMG, JP, RPW, ML, JM, JR, TB-G, MH., Visualization: RMG, JP. Funding acquisition: AA, BMN, CD, DMS, CE, ELCS, FQ, FR, HW, KE, KY, LB, MC, MM, NG, PGR, RPW, RS, SAL, SC, VS. Project administration: RPW, RMG. Writing – original draft: RPW, RMG. Writing – review & editing: all authors.

## DECLARATION OF INTERESTS

The authors declare that they have no competing interests.

## References

1. Fernandez PA (2014) Reasoning and the Unity of Aristotle's Account of Animal Motion. *Oxf Stud Anc Philos* 47
2. Hooten MB, Johnson DS, McClintock BT, Morales JM (2017) Animal movement: statistical models for telemetry data. CRC
3. Nathan R et al (2008) A movement ecology paradigm for unifying organismal movement research. *Proceedings of the National Academy of Sciences* 105, 19052–19059
4. Kays R, Crofoot MC, Jetz W, Wikelski M (2015) Terrestrial animal tracking as an eye on life and planet. *Science* 348:aaa2478
5. Nathan R et al (2022) Big-data approaches lead to an increased understanding of the ecology of animal movement. *Science* 375:eabg1780. <https://doi.org/doi:10.1126/science.abg1780>
6. Turchin P (1998) Quantitative analysis of movement: measuring and modeling population redistribution in animals and plants. Sinauer Associates
7. Munden R et al (2021) Why did the animal turn? Time-varying step selection analysis for inference between observed turning-points in high frequency data. *Methods Ecol Evol* 12:921–932
8. Nolet BA, Mooij WM (2002) Search paths of swans foraging on spatially autocorrelated tubers. *J Anim Ecol*, 451–462
9. Gunner RM et al (2021) Dead-reckoning animal movements in R: a reappraisal using Gundog. *Tracks. Anim Biotelem* 9:1–37
10. Gunner RM et al (2021) How often should dead-reckoned animal movement paths be corrected for drift? *Anim Biotelem* 9:1–22
11. Potts JR et al (2018) Finding turning-points in ultra-high-resolution animal movement data. *Methods Ecol Evol* 9:2091–2101
12. Wilson R et al (2013) Turn costs change the value of animal search paths. *Ecol Lett* 16:1145–1150. <https://doi.org/https://doi.org/10.1111/ele.12149>

13. Voigt CC, Holderied MW (2012) High manoeuvring costs force narrow-winged molossid bats to forage in open space. *J Comp Physiol B* 182:415–424
14. Scharf I, Kotler B, Ovadia O (2009) Consequences of food distribution for optimal searching behavior: an evolutionary model. *Evol Ecol* 23:245–259
15. Peters RH, Peters RH (1986) *The ecological implications of body size*, vol 2. Cambridge University Press
16. *Cognitive load theory*. (Cambridge University Press, (2010))
17. Kempton JA et al (2022) Optimization of dynamic soaring in a flap-gliding seabird affects its large-scale distribution at sea. *Sci Adv* 8:eabo0200
18. Shepard EL et al (2013) Energy Landscapes Shape Animal Movement Ecology. *Am Nat* 182:298–312. <https://doi.org/10.1086/671257>
19. Biewener AA (1990) Biomechanics of mammalian terrestrial locomotion. *Science* 250:1097–1103
20. Wall J, Douglas-Hamilton I, Vollrath F (2006) Elephants avoid costly mountaineering. *Curr Biol* 16:R527–R529
21. Wilson RP et al (2021) Path tortuosity changes the transport cost paradigm in terrestrial animals. *Ecography* 44:1524–1532
22. Taylor CR, Caldwell SL, Rowntree V (1972) Running up and down hills: some consequences of size. *Science* 178:1096–1097. <https://doi.org/10.1126/science.178.4065.1096>
23. Wilson RP et al (2015) Mass enhances speed but diminishes turn capacity in terrestrial pursuit predators. *Elife* 4:e06487
24. Williams HJ et al (2020) Physical limits of flight performance in the heaviest soaring bird. *Proceedings of the National Academy of Sciences* 117, 17884–17890 <https://doi.org/https://doi.org/10.1073/pnas.1907360117>
25. Gunner RM et al Examination of head versus body heading may help clarify the extent to which animal movement pathways are structured by environmental cues? *Movement Ecology* ((in review))
26. Bailey JD et al (2021) Micropersonality traits and their implications for behavioral and movement ecology research. *Ecol Evol* 11:3264–3273
27. Vickers NJ (2000) Mechanisms of animal navigation in odor plumes. *Biol Bull* 198:203–212
28. Dall SR, Giraldeau L-A, Olsson O, McNamara JM, Stephens DW (2005) Information and its use by animals in evolutionary ecology. *Trends Ecol Evol* 20:187–193
29. Proekt A, Banavar JR, Maritan A, Pfaff DW (2012) Scale invariance in the dynamics of spontaneous behavior. *Proceedings of the National Academy of Sciences* 109, 10564–10569 <https://doi.org/doi:10.1073/pnas.1206894109>
30. Williams HJ et al (2020) Physical limits of flight performance in the heaviest soaring bird. *Proceedings of the National Academy of Sciences* 117, 17884–17890
31. Goodale E, Beauchamp G, Magrath RD, Nieh JC, Ruxton G (2010) D. Interspecific information transfer influences animal community structure. *Trends Ecol Evol* 25:354–361

32. Dorfman A, Hills TT, Scharf I (2022) A guide to area-restricted search: a foundational foraging behaviour. *Biol Rev* 97:2076–2089
33. Fagan WF et al (2013) Spatial memory and animal movement. *Ecol Lett* 16:1316–1329
34. Bartumeus F, da Luz MGE, Viswanathan GM, Catalan J (2005) Animal search strategies: a quantitative random-walk analysis. *Ecology* 86:3078–3087
35. Mueller T, Fagan WF (2008) Search and navigation in dynamic environments—from individual behaviors to population distributions. *Oikos* 117:654–664
36. Barraquand F, Benhamou S (2008) Animal movements in heterogeneous landscapes: identifying profitable places and homogeneous movement bouts. *Ecology* 89:3336–3348
37. Kareiva P, Odell G (1987) Swarms of predators exhibit preytaxis if individual predators use area-restricted search. *Am Nat* 130:233–270
38. Weimerskirch H, Pinaud D, Pawlowski F, Bost C-A (2007) Does prey capture induce area-restricted search? A fine-scale study using GPS in a marine predator, the wandering albatross. *Am Nat* 170:734–743
39. Llobera M, Sluckin TJ, Zigzagging (2007) Theoretical insights on climbing strategies. *J Theor Biol* 249:206–217
40. Codling EA, Plank MJ, Benhamou S (2008) Random walk models in biology. *J Royal Soc interface* 5:813–834
41. Humphries NE et al (2010) Environmental context explains Lévy and Brownian movement patterns of marine predators. *Nature* 465:1066–1069. <https://doi.org/10.1038/nature09116>
42. Hodel FH, Fieberg JR (2022) Circular–linear copulae for animal movement data. *Methods Ecol Evol* 13:1001–1013
43. Harel R et al (2022) Life in 2.5D: Animal Movement in the Trees. *Front Ecol Evol* 10. <https://doi.org/10.3389/fevo.2022.801850>
44. Boulton VL et al (2018) Individual-based modelling of elephant population dynamics using remote sensing to estimate food availability. *Ecol Model* 387:187–195
45. Chudzinska M et al (2021) Agent-based model describing movement of marine central-place foragers. *Ecol Model* 440:109397. <https://doi.org/https://doi.org/10.1016/j.ecolmodel.2020.109397>. AgentSeal
46. Railsback SF, Grimm V (2019) *Agent-Based and Individual-Based Modeling: A Practical Introduction, Second Edition* Princeton University Press
47. Shepard DB, Kuhns AR, Dreslik MJ, Phillips CA (2008) Roads as barriers to animal movement in fragmented landscapes. *Anim Conserv* 11:288–296
48. Pedersen M, Poulsen E (1991) Avian response to the implementation of the Tjaereborg wind turbine at the Danish Wadden Sea. *Danske Vildtundersoegelser (Denmark)*
49. Thurfjell H, Ciuti S, Boyce MS (2014) Applications of step-selection functions in ecology and conservation. *Mov Ecol* 2:4. <https://doi.org/10.1186/2051-3933-2-4>

50. Shaw AK (2020) Causes and consequences of individual variation in animal movement. *Mov Ecol* 8:12
51. Kaidarova A, Geraldi N, Wilson RP, Kosel J, Meekan MG, Eguilez VM, Hussein MM, Shamim A, Liao H (2023) Duarte, C. Wearable sensors for monitoring marine environments and their inhabitants. *Nat Biotechnol*
52. Wilson RP, Shepard E, Liebsch N (2008) Prying into the intimate details of animal lives: use of a daily diary on animals. *Endanger Species Res* 4:123–137.  
<https://doi.org/https://doi.org/10.3354/esr00064>

## Figures

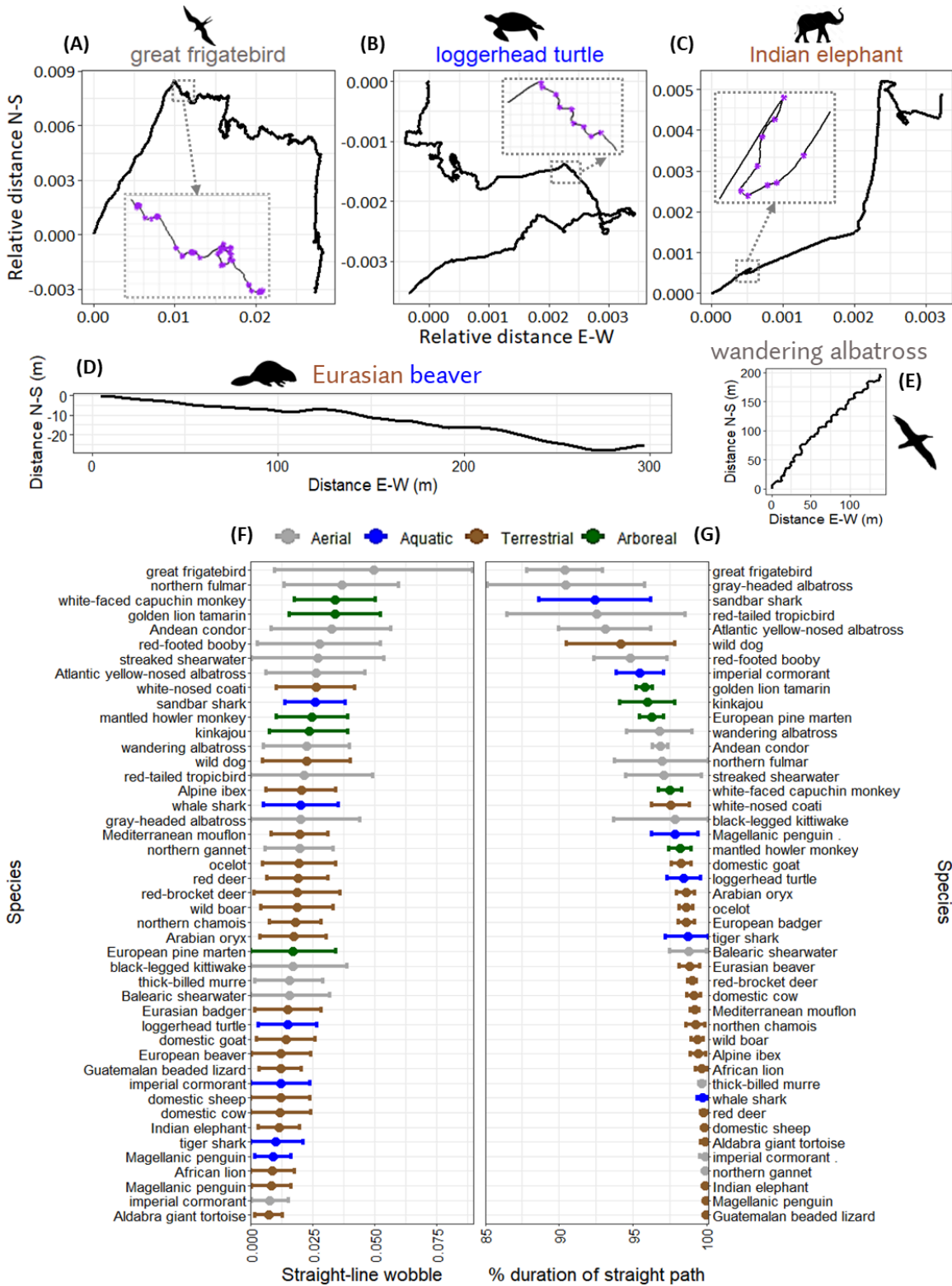


**Figure 1**

**Vertebrate movement paths are primarily composed of straight-line sections.** (A-C) Examples of movement trajectories reconstructed using data (>5 h) from species with different lifestyles and using the lifestyle indicated when the data were taken; aerial (great frigatebird, *Fregata minor*), aquatic (loggerhead turtle, *Caretta caretta*), and terrestrial (Indian elephant, *Elephas maximus indicus*). Identified turn points are shown in the inserts as purple stars. (D and E) Minor deviations in path segments

(wobble), defined nonetheless as straight-line, from a Eurasian beaver, *Castor fiber* and a wandering albatross, *Diomedea exulans*, respectively, where the former illustrates general wobble, while the latter is due to the sinusoidal movement that procellariiforms use during dynamic soaring. (F) Mean ( $\pm 1$  SD) straight-line wobble (for calculations see Supplementary text 2) of our study species and (G) mean percentage of the total path duration that is estimated to be straight-line travel (defined as having an average deviation of less than 10% from a straight line – see Supplementary text 2). The colour coding of species in the last two figures is based on their dominant mode of locomotion/lifestyle (grey = aerial, blue = aquatic, brown = terrestrial, green = arboreal). Note, however, there are exceptions in certain cases. For example, data for the Eurasian beaver, *Castor fiber*, encompassed both terrestrial and aquatic movement, white-nosed coatis, *Nasua narica*, occasionally engage in arboreal movement, and the data for Magellanic penguins, *Spheniscus magellanicus*, and imperial cormorants, *Leucocarbo atriceps*, were divided into aquatic and terrestrial phases (for the former), and aerial and aquatic phases (for the latter) stages, each of which was analysed independently.

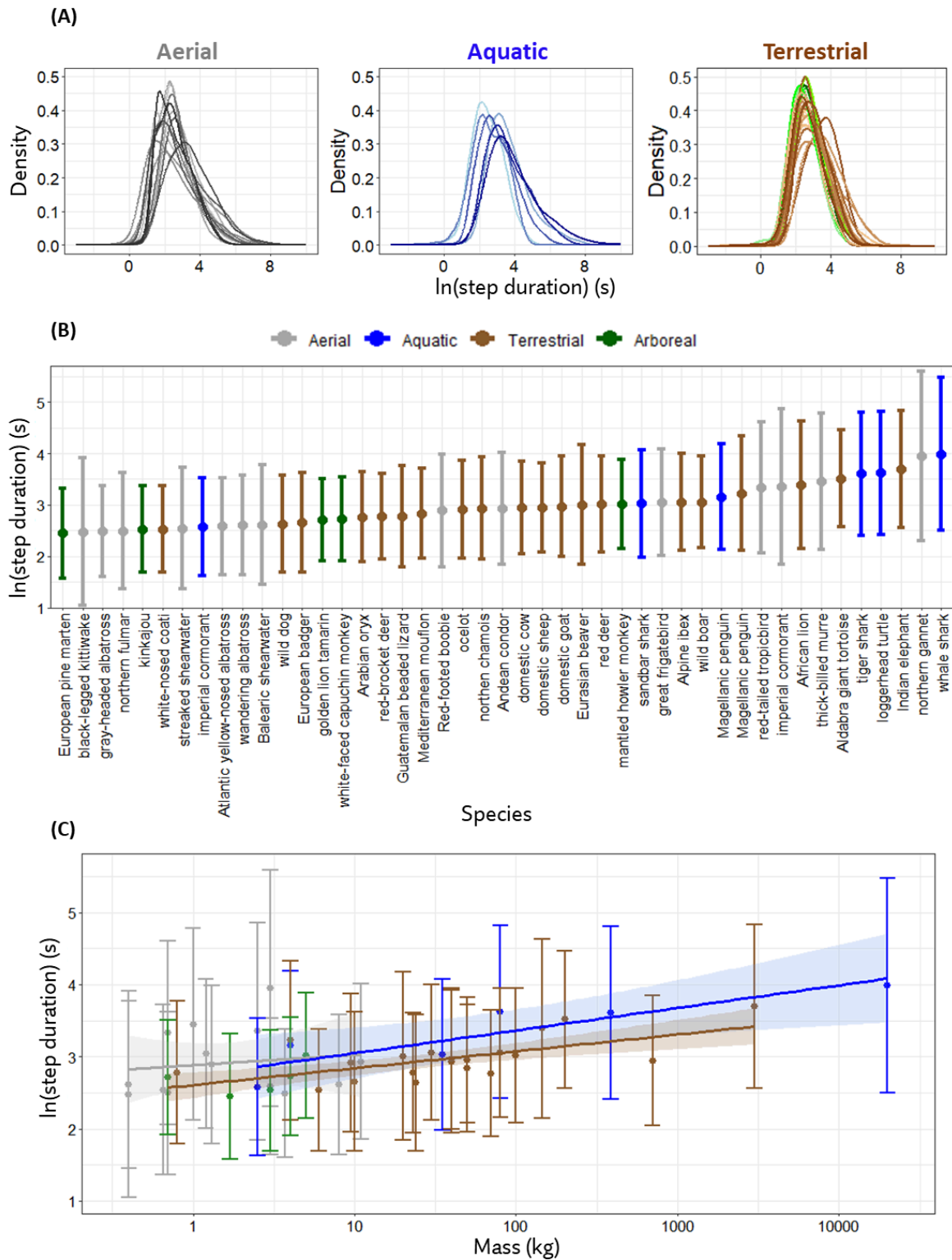


**Figure 2**

**Fundamental step durations vary with lifestyle and animal mass.** (A) Frequency distributions of  $\ln(\text{step duration})$  for the different species used in this study, color-coded according to their dominant mode of locomotion; aerial, aquatic or terrestrial (arboreal species are combined with terrestrial species in panel A). Distinct shades of each colour represent different species. (B)  $\ln(\text{step duration})$  by species and lifestyle/travel mode ( $\pm 1$  SD). (C) Relationship between  $\ln(\text{step duration})$  and species body mass across

different lifestyle/travel mode ( $\pm 1$  SD). Note, even though arboreal species (green) are represented with a distinct colour to terrestrial species (brown), they are grouped together for regression analysis (panel C) due to the limited sample size (for sample sizes of each species, see Table S1).

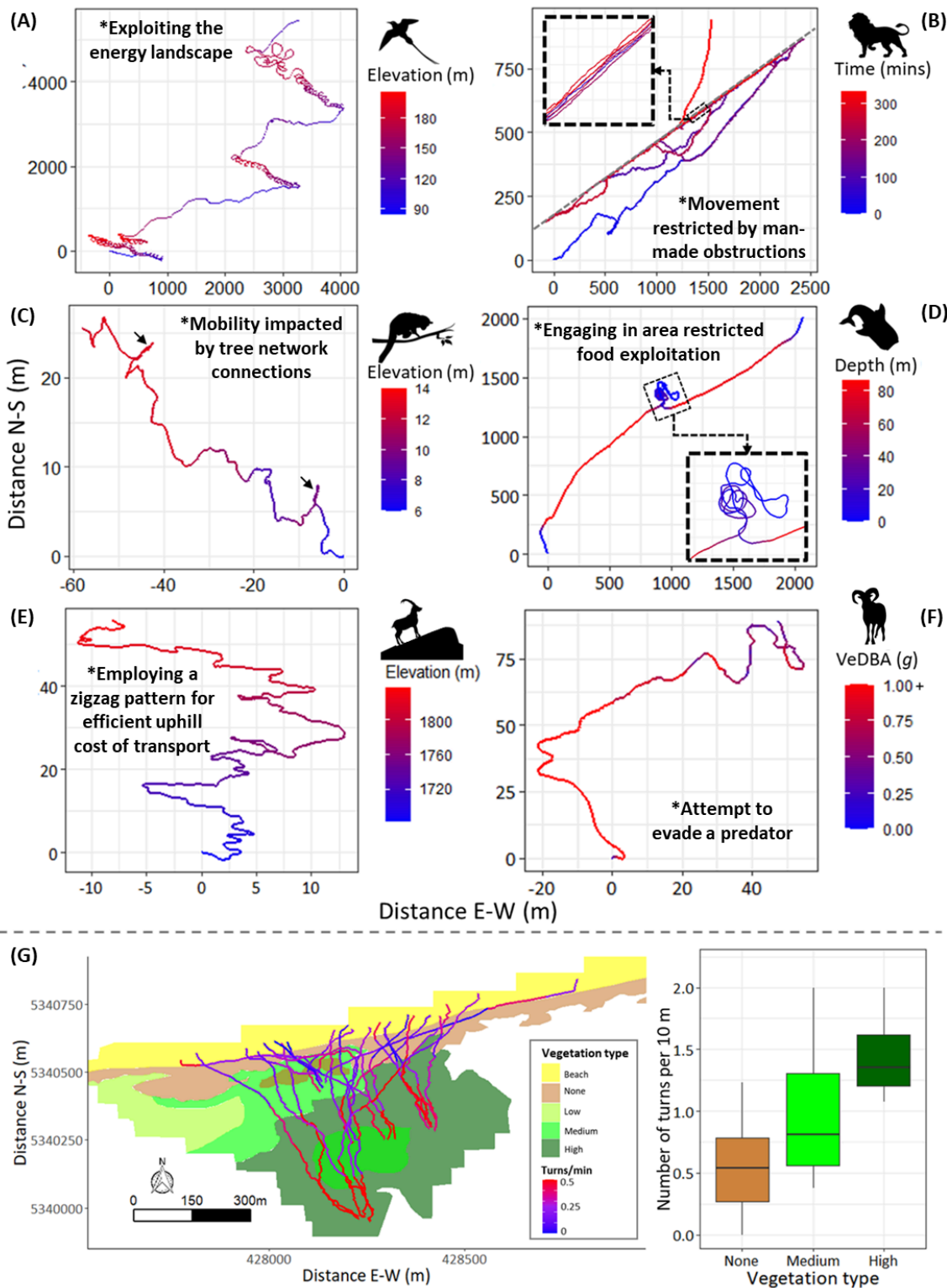


**Figure 3**

**Unveiling the reasons behind turning point selection in animal paths.** Path structures showing turns in animals exhibiting different behaviours according to environmental context. (A) A red-tailed tropicbird,

*Phaethon rubricauda*, changing direction to exploit thermals, (B) an African lion, *Panthera leo*, that had its progression constrained by a fence bounding its National Park [the animal moves repeatedly up and down the fence and eventually finds a way through], (C) a climbing kinkajou, *Potos flavus*, moves along a branch until the branch ends with no vegetation allowing it to continue in its preferred direction [about-turn points shown by arrows], (D) a whale shark, *Rhincodon typus*, terminates directional travel with extensive turning to exploit a prey patch, (E) an Alpine ibex, *Capra ibex*, uses a zig-zag movement path to ascend a slope, thereby saving energy<sup>39</sup> and (F) a Mediterranean mouflon, *Ovis gmelini musimon*, in the last few seconds of its life runs and turns in a vain bid to escape capture by a wolf, *Canis lupus*<sup>23</sup>. (G) Shows how the incidence and extent of turns varies as animals (here Magellanic penguins, *Spheniscus magellanicus*) move through an environmentally varied landscape [each track is derived from an individual bird]. Landscape categorization (shown in G) is based on drone imagery processed via Structure-from-Motion in Agisoft Photoscan version 1.4.3. The beach landscape was decrypted by eye (characterized by steep pebble drop off), and the no-, low-, medium-, and high vegetation density types were allocated based on estimates of pixel density per gridded cell (a proxy of shrubbery extent) with ~10 m by 10 m resolution. Boxplot (boxes encompass the 25~75 % interquartile range, horizontal bars reflect the median, and whiskers extend to 1.5 times the interquartile range) were constructed using the mean values per bird and vegetation type.

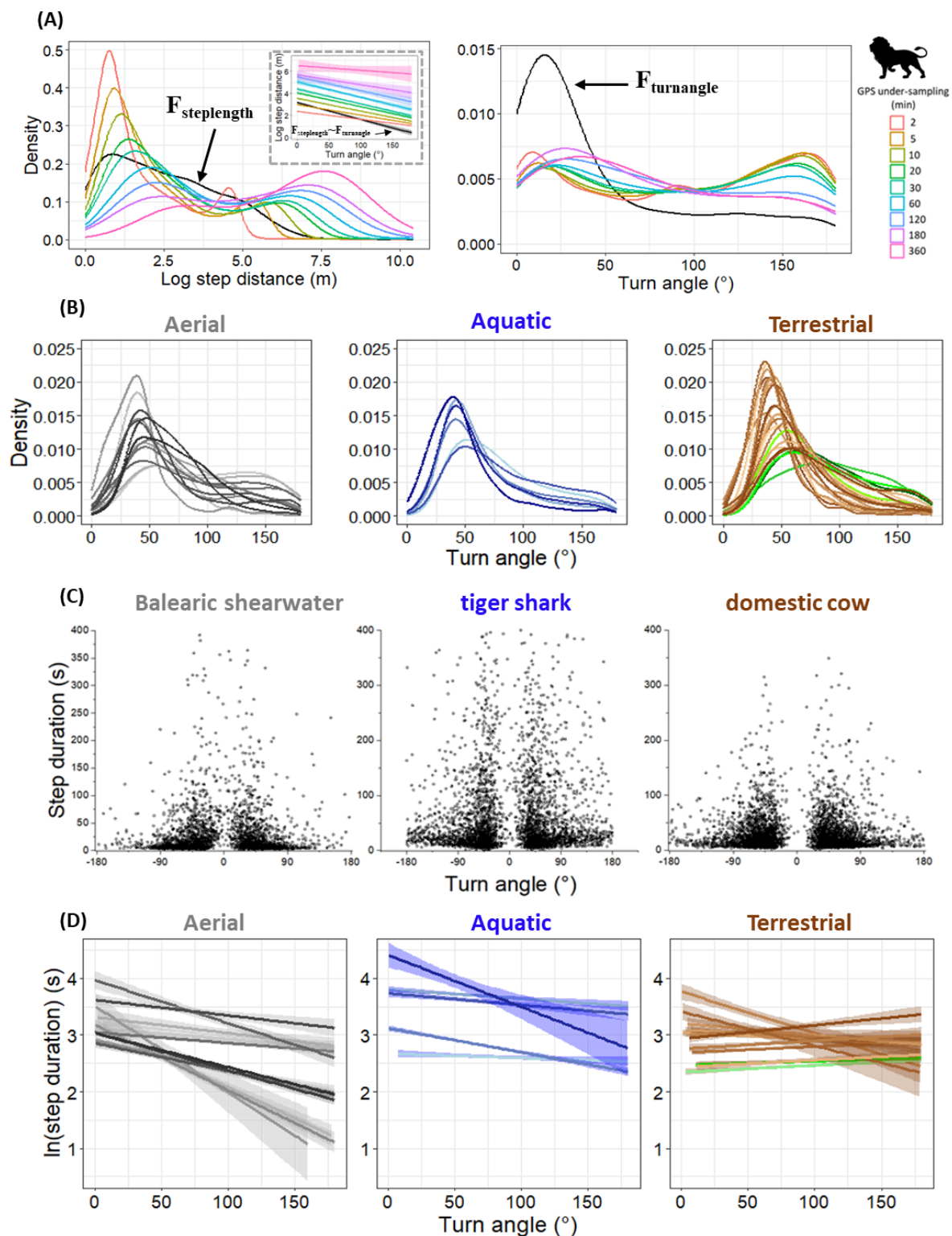
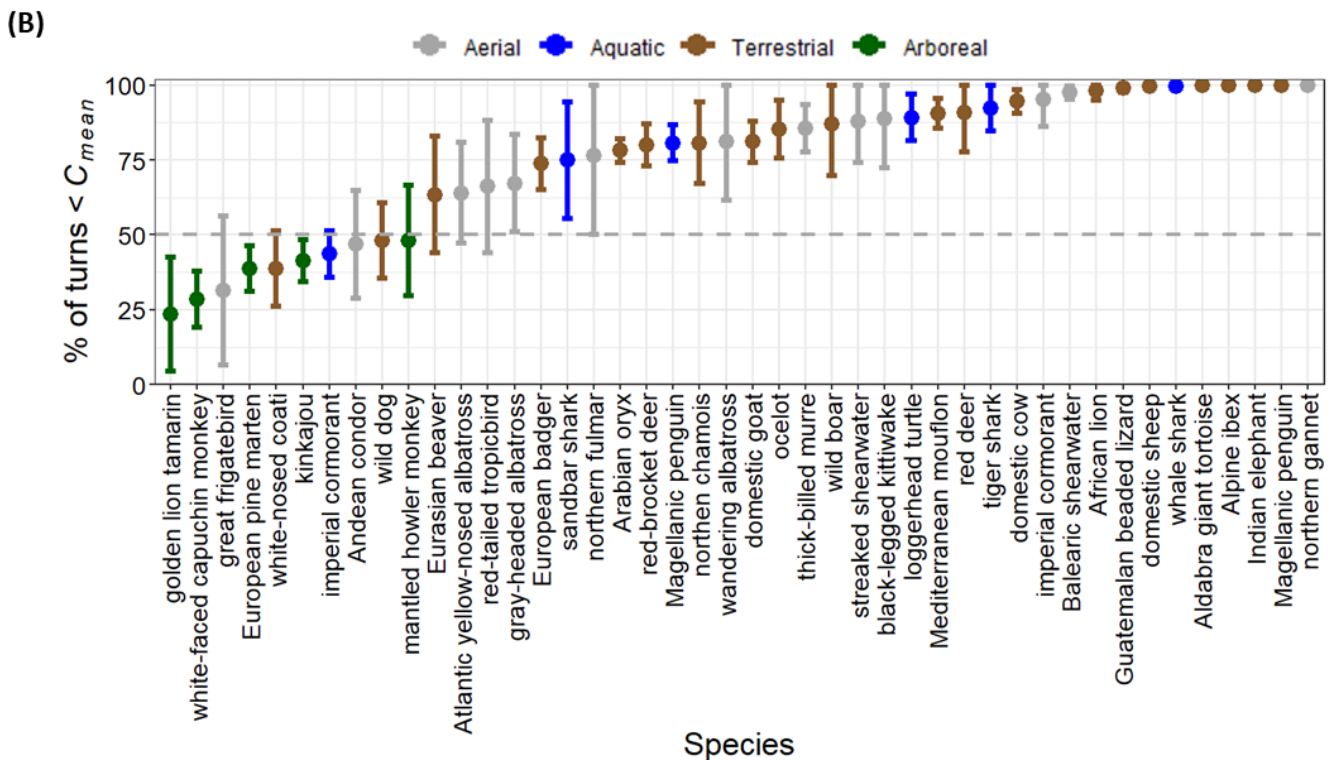
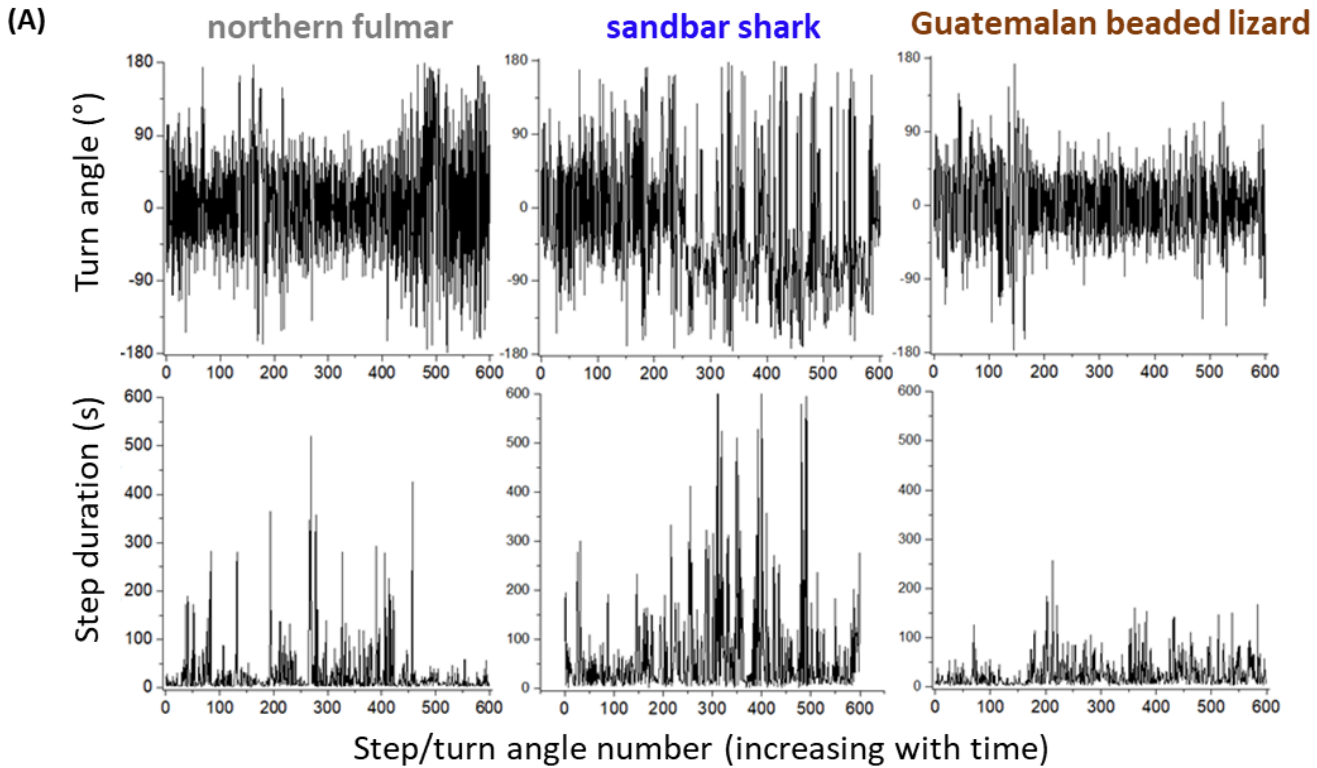


Figure 4

Turning angles, step durations and step lengths/distance and their interrelationships depend on data acquisition protocols. (A) Frequency distribution of step distances and turn angles for African lions, *Panthera leo* as a function of location data frequency [where we had high resolution GPS location data and could compare these to  $F_{stepdistance}$  and  $F_{turnangle}$  data (black lines)]. The insert shows the best fit lines between  $F_{stepdistance}$  and  $F_{turnangle}$  juxtaposed with the GPS approach based on the level of under-

sampling. (B) Frequency distribution of  $F_{\text{turnangle}}$  for the 43 species examined during movement trajectories according to lifestyle, (C) examples of how  $F_{\text{stepdurations}}$  relate to  $F_{\text{turnangles}}$  in example aerial, aquatic, and terrestrial animals and (D) best fit lines between  $F_{\text{stepduration}}$  and  $F_{\text{turnangle}}$  for those species where the two parameters were significantly correlated ( $p < 0.05$ ). The best fit lines are derived from linear models, and the shading around these regression lines represents the standard error. Note, in panels A, B, and D, turn angles are presented as absolute values (ranging from  $0^\circ$  to  $180^\circ$ ), and in panel C, turn angles are signed (spanning from  $-180^\circ$  to  $+180^\circ$ ).



**Figure 5**

**Fundamental step durations and Fundamental turn angles do not occur uniformly at random over time.**

(A) Examples of changing  $F_{\text{stepduration}}$  and  $F_{\text{turnangles}}$  over time consisting of 600 sequential steps in data for three species representing aerial, aquatic, and terrestrial lifestyles/movement, showing how there are clear periods of time when the animals adopt particular step durations and/or particular turn angles. (B) The percentage of turns that are lower than the mean circular standard deviation (the y-axis shows  $C_{\text{mean}}$ ); species with 95% confidence intervals not crossing below the dashed line exhibit patterns significantly deviating from uniform randomness (if a species is turning uniformly at random, we would expect it to have about 50% of the CSD time series below  $C_{\text{mean}}$  [see Supplementary text 2 and Table S2 for details]).

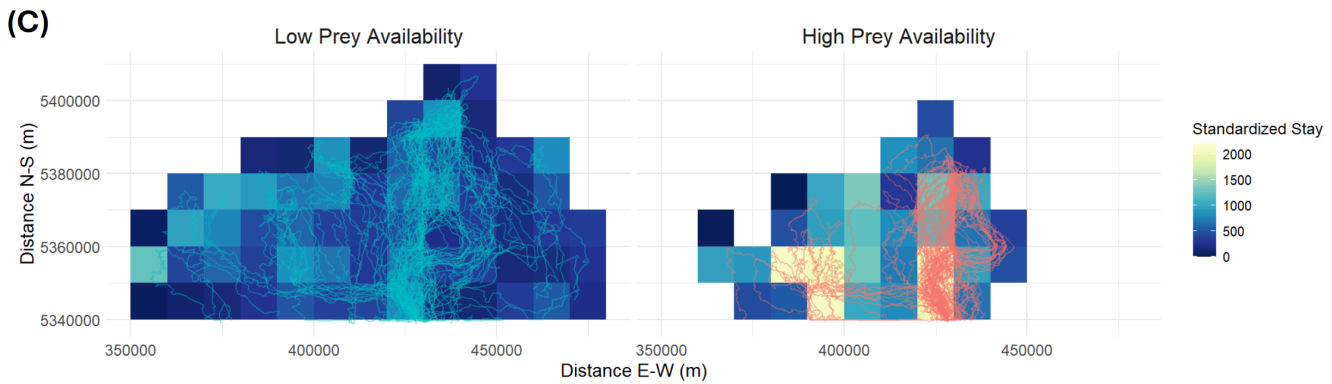
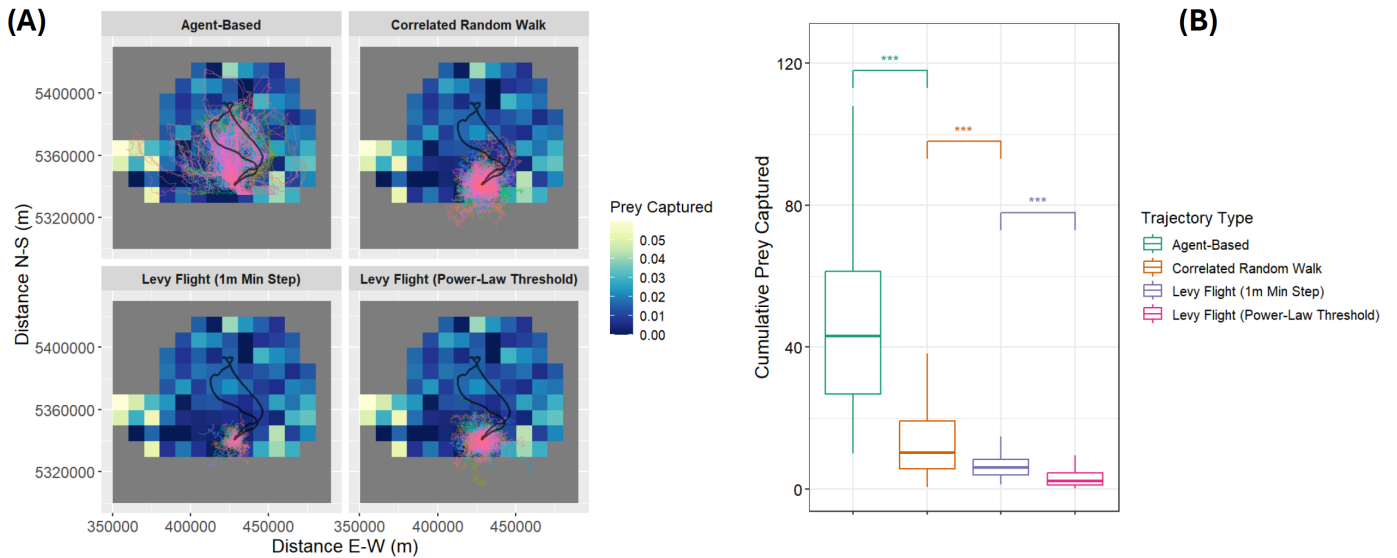


**Figure 6**

**$F_{\text{stepdistance}}$  and  $F_{\text{turnangles}}$  incorporating spatially linked heading information enhance predictions of animal movement paths.**

(A) The movement path of 300 agents simulating Magellanic penguins during single foraging trips from their breeding colony, compared to agents using correlated random walk and Lévy flight models. The black path represents an example of an actual penguin movement for comparison. (B) The predicted total number of prey items captured by each movement model used in (A). Boxes represent the interquartile range (25<sup>th</sup>-75<sup>th</sup> percentiles), horizontal bars indicate the median,

and whiskers extend to 1.5 times the interquartile range. Asterixis denote significant pairwise differences ( $P < 0.001$ , Wilcoxon signed-rank tests). (C) Predicted foraging movements of 50 agents simulating penguins using  $F_{\text{stepdistance}}$  and  $F_{\text{turnangle}}$  based on two different simulated prey density distributions. Note that the low prey distribution results in reduced time spent per cell and a substantial increase in the overall area prospected.

## Supplementary Files

This is a list of supplementary files associated with this preprint. Click to download.

- [SupplementaryInformation.docx](#)